Journal of Luminescence, 2003, 104 (1-2) : 65-76. http://dx.doi.org/10.1016/S0022-2313(02)00665-8

Luminescence Properties of Sm^{2+}-Activated Barium Chloroborates

Qinghua Zeng[a], Nathan Kilah[a], Mark Riley[a] and Hans Riesen[b]

[a] Department of Chemistry, School of Molecular and Microbial Sciences, The University of Queensland, St. Lucia, Qld. 4072, Australia
[b] School of Chemistry, University College, The University of New South Wales, Australian Defence Force Academy, Canberra, ACT 2600, Australia

Abstract

The luminescence properties of Sm^{2+}-activated stoichiometric and non-stoichiometric $Ba_2B_5O_9Cl$ were investigated from 16 to 450 K. In stoichiometric $Ba_2B_5O_9Cl$, the emission spectra of Sm^{2+} are composed of $4f^6 \rightarrow 4f^6$ transitions over the 16–450 K temperature range studied. Luminescence was observed from Sm^{2+} in four inequivalent cationic sites at 16 K and two inequivalent sites at room temperature. In the non-stoichiometric compound, the emission is characterized by $4f^6 \rightarrow 4f^6$ transitions at low temperature and $4f^5 5d^1 \rightarrow 4f^6$ transitions at high temperature. The Sm^{2+} doped into the Ca^{2+} and Sr^{2+} analogues in the $M_2B_5O_9Cl$ series shows the broad band $4f^5 5d^1 \rightarrow 4f^6$ luminescence in both the stoichiometric and non-stoichiometric compounds due to the increased ligand field caused by the smaller ionic radii of the metal ions.

Keywords: Samarium(II); $CA_2B_5O_9Cl$; $Sr_2B_5O_9Cl$; $Ba_2B_5O_9Cl$

1. Introduction

The luminescence of divalent samarium ions is sensitive to the crystalline environment of the lattice site that it occupies. The relative position of the lowest-lying $4f^5 5d^1$ excited states and the $4f^6\ ^5D_0$ level governs whether the emission displays $4f^6 \rightarrow 4f^6$ sharp line and/or $4f^5 5d^1 \rightarrow 4f^6$ broad band features. The position of the excited $4f^5 5d^1$ levels is dependent on several factors such as the crystal field strength, the coordination number and the covalence of the bonds. The excited ^5D_J (J=0,1,…) levels are relatively independent of their surroundings due to the shielding of the 4f electrons by the 5s and 5p electron shell. The temperature can also affect the emission features of Sm^{2+}: at low temperatures sharp lines of the $4f^6 \rightarrow 4f^6$ transitions will more likely be observed, while at high temperatures the $4f^5 5d^1$ energy level can be thermally populated and the broad band of the strongly allowed $4f^5 5d^1 \rightarrow 4f^6$ transitions can appear.

Luminescence of Sm^{2+} ions in solids has attracted much attention in recent years [1]. The alkaline earth haloborates $M_2B_5O_9X$ (M=Ca^{2+}, Sr^{2+}, Ba^{2+}; X=Cl, Br) activated with rare earth ions were reported to show highly efficient photostimulated luminescence and thermoluminescence after X-ray or γ-ray irradiation, features that may have application in storage phosphors for X-ray imaging and thermal-neutron detection [2 and 3]. The closely related structures of $M_2B_5O_9Cl$ are either orthorhombic (Pnn2) for M=Ca or tetragonal ($P4_22_12$) for M=Sr, Ba, Eu [4, 5 and 6]. The three-dimensional single-crystal structures have been determined for $Ca_2B_5O_9Cl$ [5] and $Eu_2B_5O_9Br$ [6], both of which crystallize in the Pnn2 space group. The structures consist of a three-dimensional $(B_5O_9)_\infty$ network in which three unique BO_4 tetrahedra and two unique BO_3 triangles are linked together. The metal ions can occupy two different C_1 crystallographic sites in the host (at room temperature), and in each case the ion is surrounded by seven oxygen and two halide atoms. The actual coordination geometry of the two metal sites is that of a distorted heptagonal bipyramid, with the two halide ions at the axial positions and equatorial O atoms at the joint of the bipyramid. The two axial halides bridge to neighbouring bipyramids. The metal and halide ions are located alternately along the tunnels of the $(B_5O_9)_\infty$ network, forming linear chains along the $a-$ ($b-$) axis for site 1 (2). Thus, the metal atoms in site 1 (2) are isolated from neighbouring metal atoms by the borate units of the $(B_5O_9)_\infty$ network in b and c directions (a and c directions)

and halide atoms in the *a*-axis (*b*-axis) direction. It is generally accepted that this structure and those of $M_2B_5O_9Cl$ (M=Ca, Sr, Ba) do not significantly differ, notwithstanding their different space groups. In both the orthorhombic (Pnn2) and tetragonal ($P4_22_12$) structures the metal occupies two inequivalent sites of both C_1 (Pnn2) or both C_2 ($P4_22_12$) symmetry. The latter is determined by systematic absences ($h00$, $h\neq 2n$; $0k0$, $k\neq 2n$) in the X-ray diffraction (XRD) powder patterns [4], indicating that the general site is not occupied.

In this paper, we report on the preparation and the luminescence properties of Sm^{2+} doped into the stoichiometric and non-stoichiometric $M_2B_5O_9Cl$ (M=Ca, Sr, Ba) host. The $Ba_2B_5O_9Cl$ system shows characteristic Sm^{2+} $4f^6\rightarrow 4f^6$ luminescence with up to 4 sites for the Sm^{2+} ion at low temperature. The emission of the Sm^{2+}-doped $Sr_2B_5O_9Cl$ host appears to be dominated by Sm^{2+}:SrB_4O_7 luminescence with subtle differences. The Sm^{2+}-doped $Ca_2B_5O_9Cl$ emission shows both sharp Sm^{3+} $4f^5\rightarrow 4f^5$ luminescence and broad band emission centred at 730 nm. We discuss the trend of the Sm^{2+} luminescence in this series of host lattices and compare it to the previously reported Sm^{2+}:$Sr_2B_5O_9Cl$ luminescence [7].

2. Experimental

The samples of stoichiometric $M_2B_5O_9Cl$ (M=Ca, Sr, Ba) doped with Sm^{2+} were prepared by firing the respective mixtures of $CaCO_3$ ($SrCO_3$, $BaCO_3$), H_3BO_3 (3 mol% excess), $CaCl_2$ ($BaCl_2.2H_2O$, $SrCl_2.6H_2O$) and Sm_2O_3 in a muffle furnace under a H_2/He (20% H_2) atmosphere. The concentration of dopant Sm_2O_3 (99.9%) was a nominal 2 mol% of M^{2+} ions. The non-stoichiometric hosts were prepared with an excess of the corresponding alkaline earth chlorides or carbonates as indicated in the text. The mixtures were first preheated to 700°C for 2 h, then ground and heated at 850°C for a further 5 h. The structures were verified by a Bruker Model D8 Advance X-ray powder diffractometer with an SOL-X EDS detector using Co $K\alpha$ radiation. Differential scanning calorimetry (DSC) measurements were made using a Perkin–Elmer model DSC7 instrument.

The excitation spectra (corrected for lamp output power) were recorded with a Perkin–Elmer Model LB-50B luminescence spectrometer with an 8 W (equivalent 20 kW) pulsed Xenon lamp as an excitation source at room temperature. The high-resolution emission spectra and decay times were recorded using Ar^+ ion laser excitation at 488 nm and a Spex-1702 0.75 m monochromator with a resolution of about 0.1 nm. The light was detected with an R430-02 cooled photomultiplier tube and a Stanford SR400 gated photon counter. The emission spectra were not corrected for the wavelength dependence of the detector and grating response. For the decay time measurements, an IntraAction AFM-603 acoustic optical modulator controlled by a Stanford Research DS345 function generator was used to chop the 488 nm line of the Ar^+ laser. The detected pulses were amplified by a Stanford Research SR445 amplifier for two stages and accumulated by a FastTech P7886 multichannel scaler. A Leybold closed-cycle cryostat was used for the low-temperature measurements and a purpose-built furnace for the high-temperature measurements. The measurements were controlled by LabVIEW software.

3. Results and discussion

Divalent Sm^{2+} has the $4f^6$ electron configuration, which under irradiation with UV and visible light, can be excited into the $4f^55d^1$ continuum from which the ions rapidly relax to the lowest excited state. The Sm^{2+}-doped $Ba_2B_5O_9Cl$ exhibits efficient deep red emission under UV and 488 nm excitation at room temperature. The excitation spectra of Sm^{2+} in $Ba_2B_5O_9Cl$ and $Sr_2B_5O_9Cl$ are shown in Fig. 1. The excitation spectra consist of two broad bands with maxima at ~350 and 510 nm. Some additional features are imposed on the spectrum of strontium chloroborate. The broad bands are due to transitions from the $4f^6$ ground state to the $4f^55d^1$ excited states of Sm^{2+} ions and the energy separation of ~9000 cm^{-1} corresponds to the 5d crystal field splitting. The sharper details may correspond to the additional multiplet splitting of the $4f^5$ configuration.

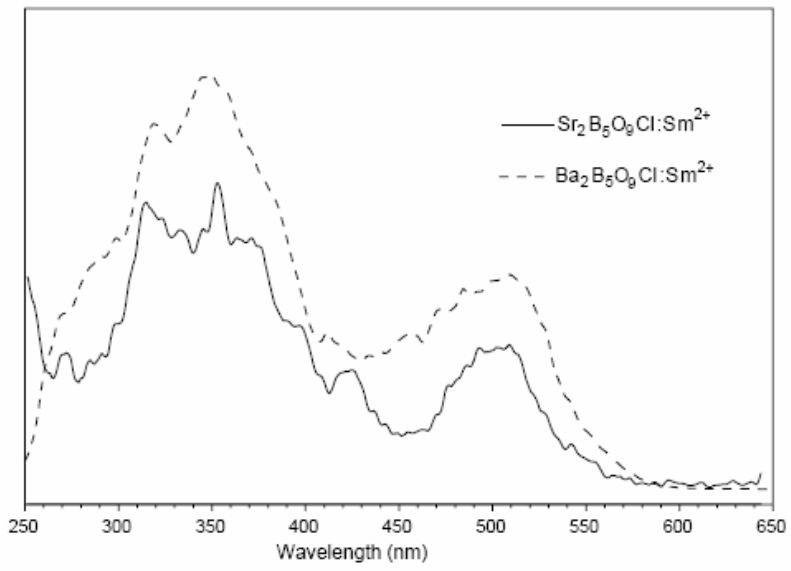

Fig. 1. Excitation spectra of Sm^{2+} in stoichiometric $Sr_2B_5O_9Cl$ and $Ba_2B_5O_9Cl$ at room temperature. The emission of the $^5D_0 \rightarrow {}^7F_0$ transition was monitored

Upon excitation into the $4f^55d^1$ states, the Sm^{2+} in $Ba_2B_5O_9Cl$ shows strongly temperature dependent luminescence from $^5D_0$ to ^7F_J levels. The emission spectra of Sm^{2+} in $Ba_2B_5O_9Cl$ were recorded in the temperature range 16–450 K and Fig. 2 depicts the spectra at these two limits. Due to spin–orbit coupling and the crystal field the ^5D_J and ^7F_J energy multiplets are split into several sublevels. Five groups of lines are observed, which correspond to the transitions between the levels of the $^5D_0$ and ^7F_J (J=0,1,2,3,4) multiplets of Sm^{2+}. At low temperature there are four strong lines in the expected region of the $^5D_0 \rightarrow {}^7F_0$ transition at 681.9, 683.2, 683.5 and 683.9 nm (designated I, II, III and IV, respectively, in Fig. 2). Since the $^5D_0$ and $^7F_0$ energy level cannot be split by the crystal field, the number of the $^5D_0 \rightarrow {}^7F_0$ peaks corresponds to the number of inequivalent sites occupied by Sm^{2+} in the host lattice. Four sites are, therefore, available for the Sm^{2+} ions at 16 K in this host. The degeneracy of the $^7F_1$ levels has been lifted and nine peaks are observed in the spectral region of the $^5D_0 \rightarrow {}^7F_1$ transitions from 16 to 80 K. The ($2J$+1=3) degeneracy of the $^7F_1$ multiplet is expected to be fully removed for Sm^{2+} ions occupying a C_2 or C_1 crystallographic site. So it is presumed that 3 of the 12 expected peaks are weak or overlapping with the 9 observed peaks.

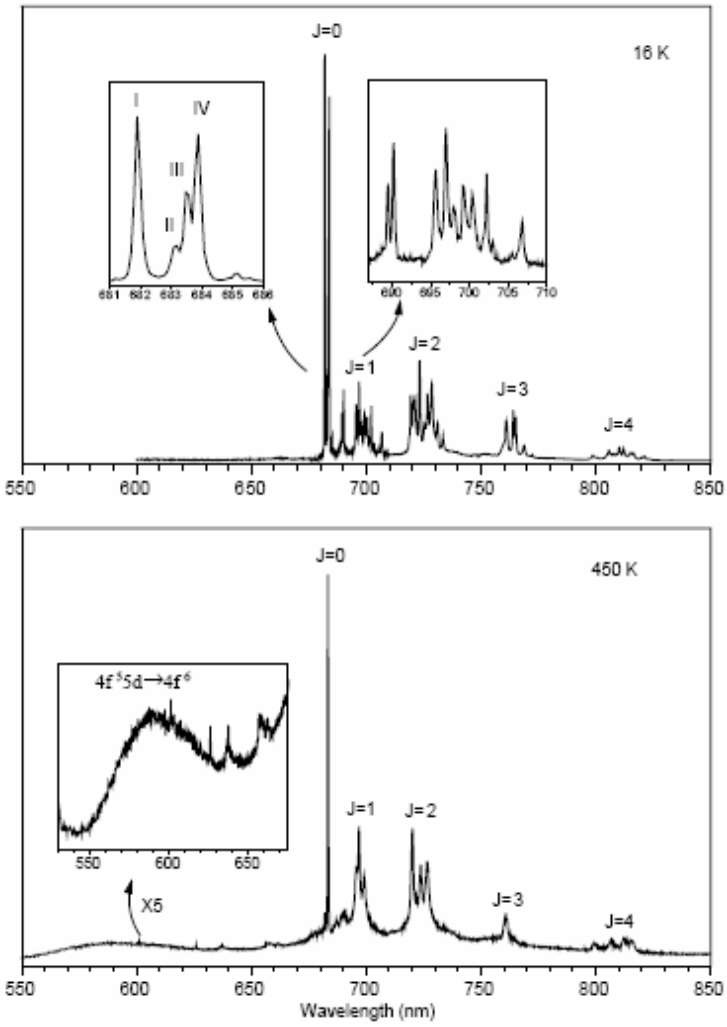

Fig. 2. Emission spectra in the region of the $^5D_0 \rightarrow {}^7F_J$ transitions of Sm^{2+} in stoichiometric $Ba_2B_5O_9Cl$ at 16 and 450 K. The spectra were excited by using 488 nm Ar^+ laser light.

The integrated intensity of the $^5D_0 \rightarrow {}^7F_0$ and $^5D_0 \rightarrow {}^7F_1$ transitions is strongly temperature dependent as shown in Fig. 2. Firstly, we turn our attention to the temperature dependence of the $^5D_0 \rightarrow {}^7F_0$ transitions in Fig. 3. The emission from site I has the highest intensity among all the transitions at 16 K and it slightly decreases in intensity with increasing temperature up to 80 K. The peak of site II also decreases and disappears at about 80 K, while the intensity of the emission from site III slowly increases. The emission intensity from site IV decreases at all temperatures with the largest variation between 80 and 150 K. The emission from site IV is completely quenched at 240 K, while the emission intensities of sites I and III increase until 300 and 240 K, respectively. This behaviour may be indicative of excitation energy transfer between the sites. However, the transitions of sites II, III and IV are all within ~20 cm^{-1} and hence energy transfer would not be *mono*-directional. For example, phonon-assisted energy transfer would be as likely from site II to site III as vice versa at 80 K. Furthermore, the relatively low oscillator strength of the $^5D_0 \rightarrow {}^7F_0$ transition in conjunction with the Sm^{2+} concentration (2%) used in the present work render energy transfer an unlikely process.

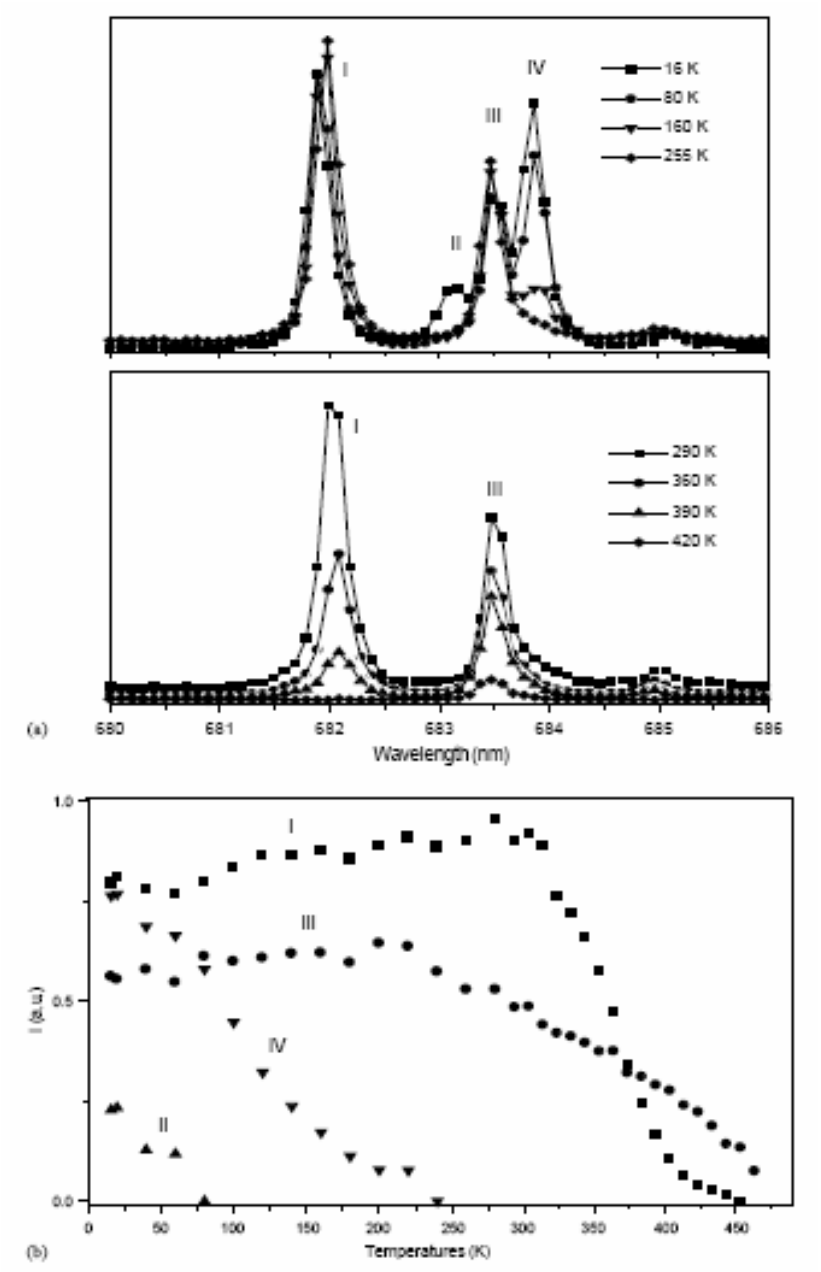

Fig. 3. (a) Temperature dependence of the $^5D_0 \rightarrow {}^7F_0$ transition of Sm^{2+} ions in different sites in stoichiometric $Ba_2B_5O_9Cl$. (b) Temperature dependence of the integrated intensities of the $^5D_0 \rightarrow {}^7F_0$ transition of the four sites.

The emission intensities of the $^5D_0 \rightarrow {}^7F_0$ transition of sites I and III start to decrease at ~300 and ~230 K. The intensity of the $^5D_0 \rightarrow {}^7F_0$ transition of Sm^{2+} of site I is higher than that of site III at room temperature but it decreases much faster as the temperature is raised. At 373 K the emission of Sm^{2+} in the two sites is almost equal; when the emission in site I is quenched at 450 K the emission from site III is still relatively strong.

Extensive measurements of the lifetimes of the $^5D_0 \rightarrow {}^7F_0$ transition in the different sites were performed from 16 to 450 K as illustrated in Fig. 4. The decay curves of the $^5D_0 \rightarrow {}^7F_0$ transition of Sm^{2+} from site I are single exponential at all temperatures. The lifetime is temperature independent with a value of around 4.5 ms from 16 to 320 K, and then it decreases with further increasing temperature until the emission is quenched at 450 K.

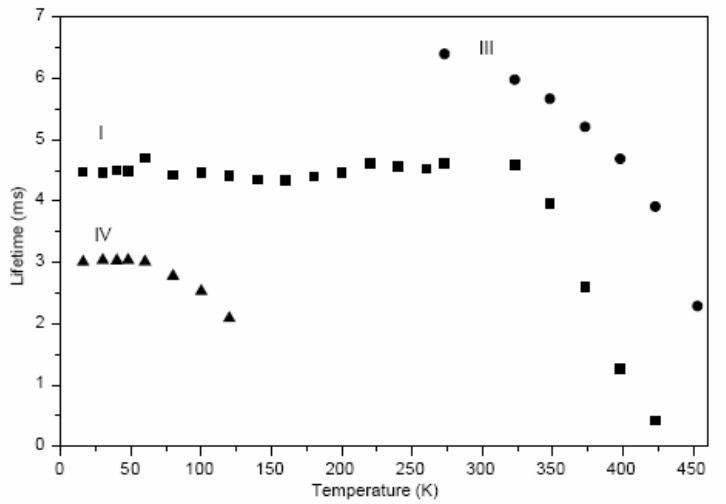

Fig. 4. Temperature dependence of the $^5D_0$ excited state lifetime of the Sm^{2+} in stoichiometric $Ba_2B_5O_9Cl$ for the four inequivalent sites.

The analysis of the temperature dependence of the excited state lifetimes of sites II, III and IV is complicated by the overlap of the emission spectra. The fluorescence decay of Sm^{2+} in site IV is single exponential with a lifetime about 3.0 ms between 16 and 70 K, then decreases to 2.0 ms at 120 K. A long tail then appears in the decay curve at higher temperature, resulting in a double exponential decay up to 240 K. The decay curves for Sm^{2+} in sites II and III are non-single exponential below 240 K. Finally, from 240 to 450 K, the fluorescence decay of site III is again single exponential and the lifetime decreases from 6.4 ms at 273 K to 2.3 ms at 450 K.

Two crystallographic sites were also observed for Eu^{2+}-doped $Ba_2B_5O_9Cl$ based on a 16 nm splitting of some broad emission at 4.2 K [8]. These authors reported that energy transfer from the higher to the lower energy site takes place via an electric dipole–dipole interaction. The emission of Eu^{2+} from sites II, III and IV may be too close to be resolved while the sharper lines of Sm^{2+} allows them to be distinguished. When the temperature is raised above 220 K, two emission peaks for the $^5D_0 \rightarrow {}^7F_0$ transition are observed in agreement with the two different sites of the room temperature crystal structure of the host [4, 5 and 6]. DSC measurements were made over the temperature range 90–300 K, but we could not detect any phase transitions. It is noted that DSC is sometimes unable to detect phase transitions if the calorimetric change is small. This is in accord with the *gradual* disappearance of the sites II and IV emission: abrupt quenching of emission would be expected for a proper structural phase transition. The fact that the number of inequivalent sites varies at different temperatures can be explained as follows. The ionic radius of Sm^{2+} ion (136 pm) is smaller than that of the Ba^{2+} ion (152 pm) [9]. Thus, Sm^{2+} may take up different equilibrium positions when it substitutes for Ba^{2+} in the host lattice. It may be that the Cl ions can more easily relax compared to the relatively rigid borate framework. Two different relaxed distortions in each site, with one being *stabilized* at low temperature would then give rise to the four $^5D_0 \rightarrow {}^7F_0$ transition lines observed at low temperature. It is possible that the gradual quenching of the luminescence from sites II and IV at low temperature is due to a structural relaxation effect.

The thermal behaviour of the $^5D_0 \rightarrow {}^7F_0$ transition of Sm^{2+} facilitates the assignment of the emission lines of the $^5D_0 \rightarrow {}^7F_1$ transitions to the different luminescent sites. Fig. 5 shows the $^5D_0 \rightarrow {}^7F_1$ emission lines at different temperatures. Three peaks at 450 K, six peaks at 240 K and nine well-separated peaks at 77 K (designated *a*,*b*,*c*,*d*,*e*,*f*,*g*,*h*,*i* in Fig. 5) are observed. Since luminescence of Sm^{2+} ions occurs only in site III at 450 K, lines *c, d* and *f* can be assigned to the $^5D_0 \rightarrow {}^7F_1$ transitions of Sm^{2+} in site III. From the spectrum at 240 K (at which the emission from sites II and IV are quenched) it follows that lines *b*,*e* and *g* are due to site I. Finally, lines *a*,*h* and *l* can be assigned to site IV. The emission spectra of the $^5D_0 \rightarrow {}^7F_1$ transitions of Sm^{2+} ions at 16 and 77 K are identical; Thus, no $^5D_0 \rightarrow {}^7F_1$ emission

peaks can be assigned to the Sm^{2+} ion in site II. The energy positions and assignment of the emission spectra of Sm^{2+} in the different sites in stoichiometric $Ba_2B_5O_9Cl$ at 16 K are summarized in Table 1.

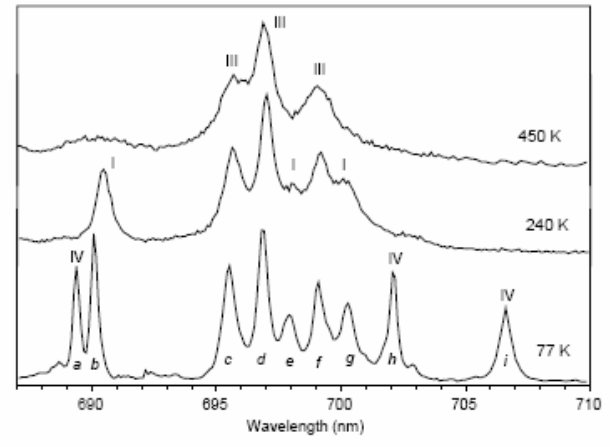

Fig. 5. Temperature dependence of the $^5D_0 \rightarrow {}^7F_1$ transitions of Sm^{2+} in stoichiometric $Ba_2B_5O_9Cl$.

Table 1. Energy levels (in cm^{-1}) of Sm^{2+} in stoichiometric $Sr_2B_5O_9Cl$, SrB_4O_7 and $Ba_2B_5O_9Cl$

Level	$Sr_2B_5O_9Cl$	SrB_4O_7	$Ba_2B_5O_9Cl$			
			I	II	III	IV
$^7F_0$	0	0	0	0	0	0
$^7F_1$						
(1)	210	211	174		252	117
(2)	278	276	336		279	379
(3)	401	397	385		326	471
$^7F_2$						
(1)	744	741				
(2)	783	782				
(3)	837	836				
(4)	?	956				
(5)	961	965				
$^5D_0$						
(1)	14,591	14,585	14,665	14,639	14,630	14,623
$^5D_1$						
(1)	15,913	15,910				
(2)	15,944	15,943				

The $^5D_1 \rightarrow {}^7F_0$ transition can be observed (insert to Fig. 2) in Sm^{2+}-doped $Ba_2B_5O_9Cl$ at around 450 K due to the thermal population of the $^5D_1$ level. In addition, a rather strong broad band with a peak at around 590 nm can be seen, resulting in a yellow emission under 488 nm excitation, at this temperature, which is characteristic of Sm^{2+} $4f^5 5d^1 \rightarrow {}^7F_J$ transitions in borates. The population of this broad band transition above a relatively narrow transition can be rationalized in terms of the Franck–Condon displacements in a configurational coordinate plot of the form given by Wickleder [10].

In addition to the strong emission lines presented in Fig. 2, additional weak lines shifted by ~70 cm^{-1} to the lower energy side of the $^5D_0 \rightarrow {}^7F_0$ transition can be observed at low temperatures. These bands are due to vibronic transitions, resulting from the electron–phonon interactions and we assign the 70 cm^{-1} mode to a lattice phonon [11].
The luminescence properties of Sm^{2+} ions in *non-stoichiometric* $Ba_2B_5O_9Cl$ and stoichiometric $Ba_2B_5O_9Cl$ are very different even though no impurity phases were detected from the XRD patterns with up to 50% excess $BaCO_3$ or $BaCl_2$. Fig. 6 depicts the luminescence spectra of Sm^{2+} in non-stoichiometric $Ba_2B_5O_9Cl$ with a 10 mol% excess of $BaCl_2$. At room temperature the emission spectrum is composed of a broad band emission with a maximum at around 700 nm and two superimposed lines at 681.9 and 683.9 nm. The luminescence spectrum was the same whether $BaCl_2$ or $BaCO_3$ was used in excess. The broad emission band corresponds most likely to the $4f^55d^1 \rightarrow 4f^6$ transition. The intensity of the broad band emission decreases with decreasing temperature and completely disappears while the intensity of the sharp line emission increases. At 77 K, only the sharp line emission that is characteristic of Sm^{2+} $4f^6 \rightarrow 4f^6$ transitions are observed (Fig. 6). It should be noted that a weak line at 683.2 nm and a strong one at 683.9 nm occur in the region corresponding to the $^5D_0 \rightarrow {}^7F_0$ transition. Neither of these peaks corresponds to luminescence of Sm^{2+} in the excess $BaCl_2$ phase, as only one line for the $^5D_0 \rightarrow {}^7F_0$ transition was observed at 687.1 nm in single-crystal $BaCl_2$ [12]. In addition, the same luminescence spectrum was observed in $Ba_2B_5O_9Cl$ with a 10 mol% excess of $BaCO_3$. These results imply that impurity phases other than $BaCl_2$ or $BaCO_3$ (which decomposes into BaO after reaction) may exist when an excess starting material is added, and XRD is unable to detect their existence.

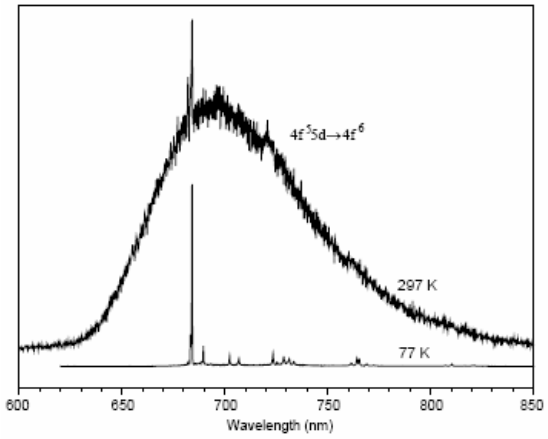

Fig. 6. Luminescence spectra of Sm^{2+} in non-stoichiometric $Ba_2B_5O_9Cl$ (using 488 nm Ar^+ laser excitation) at 77 K and room temperature.

We have also prepared Sm^{2+}-doped $Sr_2B_5O_9Cl$. The emission spectrum of Sm^{2+} at room temperature in $Sr_2B_5O_9Cl$ is presented in Fig. 7a. Four groups of lines from 680 to 800 nm can be observed corresponding to the $^5D_0 \rightarrow {}^7F_J$ (J=0,1,2,3) transitions of Sm^{2+} in the host, respectively. The spectrum is very similar to that of Sm^{2+}:SrB_4O_7 which is shown for comparison in Fig. 7b under the same conditions. The peak positions and assignments are listed in Table 1. A group of weak lines from 560 to 650 nm were observed at room temperature as shown in the inset in Fig. 7a. The three stronger and somewhat broader peaks are assigned to Sm^{3+} transitions as indicated. It is known to be quite difficult to incorporate the Sm^{3+} ion in the SrB_4O_7 lattice [13]. There are also weaker, sharper and temperature dependent peaks between 625 and 640 nm that are assigned to $^5D_1 \rightarrow {}^7F_J$ transitions. The decay of the $^5D_0 \rightarrow {}^7F_0$ transition of Sm^{2+} were measured as a function of temperature from room temperature to 450 K. All the decay curves are single exponential with a decay time of ~4.1 ms at room temperature decreasing to ~3.1 ms at 450 K.

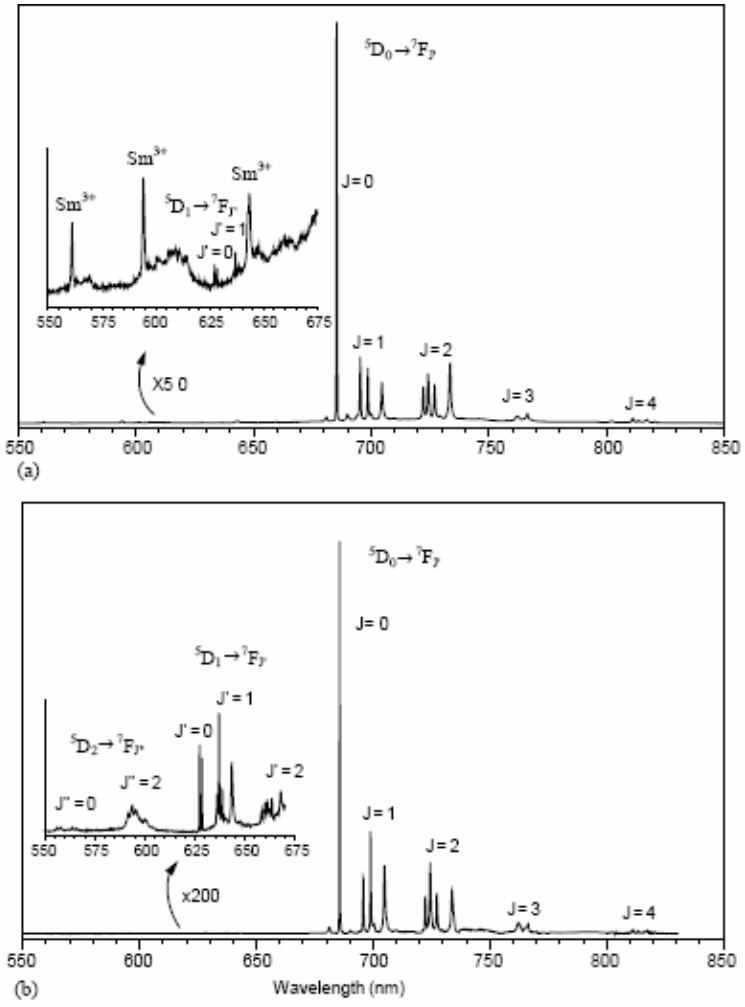

Fig. 7. Luminescence spectrum of Sm^{2+} (using 488 nm excitation) at room temperature (a) in stoichiometric $Sr_2B_5O_9Cl$ and (b) in SrB_4O_7. (The inset shows the spectrum from 550 to 660 nm on an expanded scale.)

The luminescence properties of Sm^{2+}-doped $Sr_2B_5O_9Cl$ and Sm^{2+} in SrB_4O_7 [13, 14 and 15], are quite similar: the number of the transition peaks and their positions from $^5D_{0,1}$ to ^7F_J are very close as is shown in Table 1. The repeated synthesis of Sm^{2+}:$Sr_2B_5O_9Cl$ gave the same results, and in no case could the XRD detect any XRD patterns of SrB_4O_7. Small differences of the spectra of Sm^{2+} ion in $Sr_2B_5O_9Cl$ and SrB_4O_7 are observable. First, the lifetime of the $^5D_0 \rightarrow {}^7F_0$ transition of Sm^{2+} in $Sr_2B_5O_9Cl$ is temperature dependent while in SrB_4O_7 it has an almost temperature independent [13] value of 3.5 ms; secondly, at higher temperature, a broad band with maximum at around 585 nm can be observed for Sm^{2+} in SrB_4O_7 due to thermal population [13] while no such broad band was found in $Sr_2B_5O_9Cl$. Finally, from the excitation spectra of Sm^{2+} in Fig. 1, the crystal field splitting of the 5d level in $Sr_2B_5O_9Cl$ is ~9000 cm^{-1}, compared to ~6990 cm^{-1} in SrB_4O_7 [13]. Since the geometric environments of Sm^{2+} in $Sr_2B_5O_9Cl$ and SrB_4O_7 are different, it is very unlikely to show the same luminescence spectrum in the two systems. Thus, we conclude, in spite of the small differences observed, that the emission spectrum of Sm^{2+} in $Sr_2B_5O_9Cl$ is dominated by a very small amount of SrB_4O_7 impurity. This is support by the observation that very similar spectra were obtained from $Sr_2B_5O_9Cl$ samples prepared in air to those prepared in H_2. This behaviour is similar to that observed for SrB_4O_7; whereas, the preparation of the $Ba_2B_5O_9Cl$ samples *required* a reducing H_2 atmosphere to stabilize the Sm^{2+} ion in the sample.

The luminescence of Sm^{2+} in $Sr_2B_5O_9Cl$ has also been investigated by Dotsenko et al. [7] who observed different results from those given here. The authors reported that the

emission spectrum of Sm^{2+} in $Sr_2B_5O_9Cl$ is composed of a broad band $4f^55d^1 \rightarrow 4f^6$ transition with a maximum at ~700 nm. We suspect that an excess of starting materials was probably used during their preparation process causing other phases in the resultant compound, as seen above for the preparation of $Ba_2B_5O_9Cl$. To test this, a series of Sm^{2+}-doped samples with different excesses of $SrCl_2$ and $SrCO_3$ were therefore prepared. The XRD patterns of these non-stoichiometric samples indicated that samples with excess $SrCl_2 \cdot 6H_2O$ up to 30% show the same XRD patterns as reported for $Sr_2B_5O_9Cl$. [4]. No impurity phases were detected by XRD. A further excess of $SrCl_2 \cdot 6H_2O$ resulted in peaks of $SrCl_2 \cdot 6H_2O$ appearing in the XRD patterns. (The $SrCl_2$ phase that is prepared in the non-stoichiometric compounds readily reabsorbs H_2O.)

The emission spectra of Sm^{2+} ions in the non-stoichiometric hosts are different from those of Sm^{2+} in the stoichiometric hosts, as shown in Fig. 8. In the sample with 10% excess of $SrCl_2$, the emission spectrum is composed of the sharp lines characteristic of Sm^{2+}, superimposed on a broad band. In the samples with 20% and more excess (up to 200%) of $SrCl_2$, the emission spectra of Sm^{2+} is only composed of a broad band extending from about 640 to 860 nm with a maximum at around 720 nm and a full-width at half-maximum (FWHM) of about 80 nm. These results are similar to those reported by Dotsenko et al. [7] and the emission spectra must origin from the $4f^55d^1 \rightarrow 4f^6$ transition of Sm^{2+} ions. It is noted here that the energy of this transition is more typical of Sm^{2+} in chlorides than borates. An emission line at 681.7 nm together with the $4f^55d^1 \rightarrow 4f^6$ broad emission band was observed at 80 K and assigned to the zero-phonon line of the $4f^55d^1 \rightarrow 4f^6$ transitions by the authors. This line was also found in our investigation in non-stoichiometric host at 77 K as shown in Fig. 8b. However, the sharp line emission also occurs at 16 K without the broad band emission. This indicates that this line due to the $^5D_0 \rightarrow {}^7F_0$ transition rather than being a zero-phonon line of the $4f^55d^1 \rightarrow 4f^6$ transition, since there are also transitions from $^5D_0$ to $^7F_1$ and $^7F_2$ levels, which are typical emission features of Sm^{2+}. The same emission features were observed in the samples with an excess $SrCO_3$. It is therefore uncertain whether the broad band and line emission come from the Sm^{2+} in $SrCl_2$ or from other impurity phase.

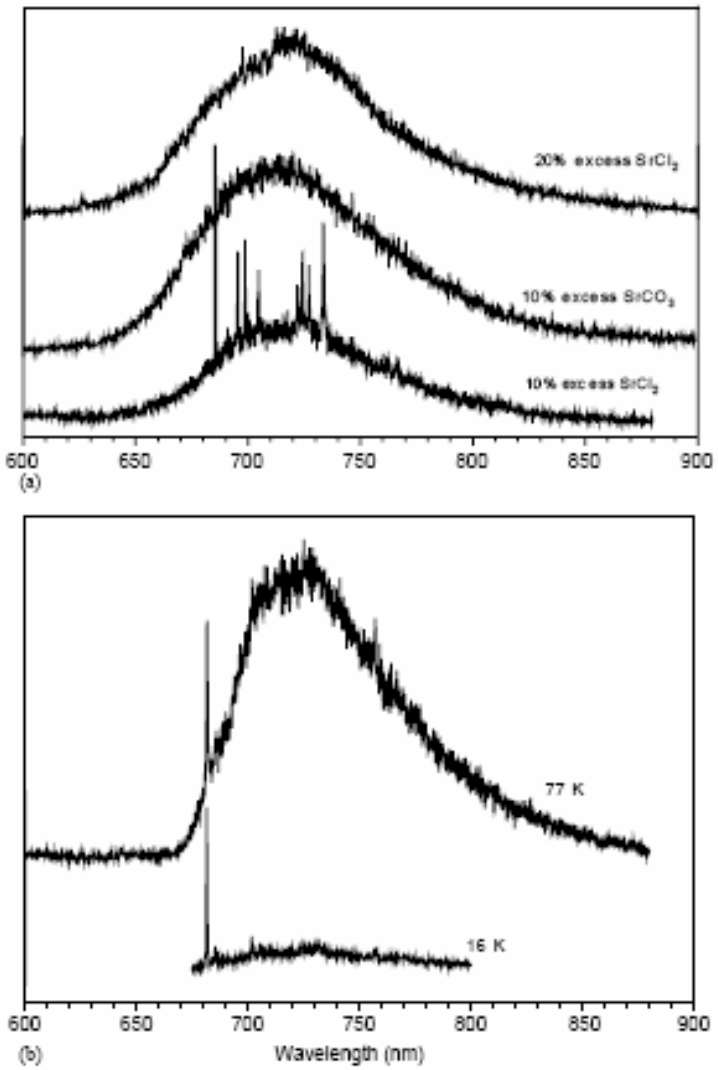

Fig. 8. Luminescence spectra of Sm^{2+} in non-stoichiometric $Sr_2B_5O_9Cl$ (using 488 nm excitation) (a) at room temperature with different excesses of starting materials, and (b) with 20% excess of $SrCl_2$ at 77 and 16 K.

The emission spectra of Sm^{2+} in $SrCl_2$ single crystals were reported by Axe et al. [16]. A broad band $4f^5 5d^1 \rightarrow 4f^6$ emission and a sharp line at 700.7 nm were observed at room temperature and at 77 K, respectively. The latter was assigned to the $^5D_0 \rightarrow {}^7F_1$ transition. No lines at around 680 nm, being a typical position for the $^5D_0 \rightarrow {}^7F_0$ transition, were observed due to the cubic site symmetry of Sm^{2+} ions in $SrCl_2$.

The luminescence of Sm^{2+} in $Ca_2B_5O_9Cl$ is shown in Fig. 9. In contrast to the other two hosts, no sharp line $4f^6 \rightarrow 4f^6$ emission of Sm^{2+} was observed at room temperature or at 77 K. The luminescence in these samples was very weak as can be seen by the relatively noisier signals. Some of weak emission can be attributed to Sm^{3+} ions, the weak broad band centred at 730 nm may have its origin in chloride impurities as discussed above.

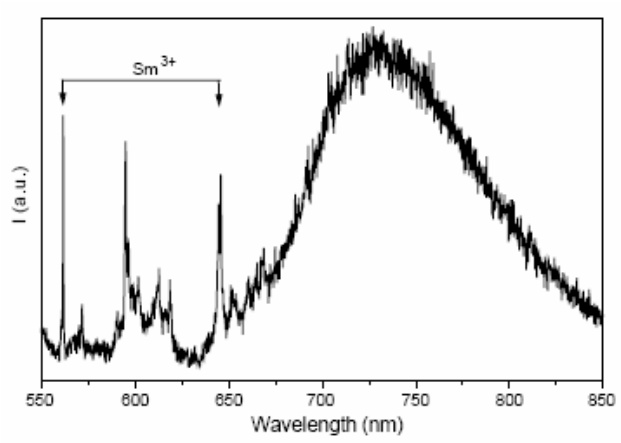

Fig. 9. Luminescence spectra of samarium-doped $Ca_2B_5O_9Cl$ (using 488 nm excitation) at room temperature. The peaks due to Sm^{3+} are indicated.

The relative position of the lowest-lying $4f^55d^1$ excited states and the $^5D_0$ level governs whether the emission displays $4f^6 \rightarrow 4f^6$ sharp line and/or $4f^55d^1 \rightarrow 4f^6$ broad band features. The trend observed in the luminescence spectra suggests that the energy gap between the $4f^55d^1$ and $^5D_0$ energy levels decreases along the series $M_2B_5O_9Cl$ (M=Ba, Sr, Ca). That is, the broad band $4f^55d^1 \rightarrow 4f^6$ emission is more readily seen for Sm^{2+} replacing a smaller cation. This is consistent with the smaller cation site imparting a larger ligand field which splits the 5d states to a greater extent. Since the $4f^55d^1$ states are at higher energy than the $^5D_0$ level (which is insensitive to the ligand field) a greater splitting will in general reduce the energy gap between the $^5D_0$ level and the lowest $4f^55d^1$ level. This trend can also be observed in trivalent lanthanides [17].

4. Conclusions

The luminescence of Sm^{2+} doped in stoichiometric and non-stoichiometric $Ba_2B_5O_9Cl$ was investigated. Four sites (I, II, III and IV) are observed for Sm^{2+} in stoichiometric $Ba_2B_5O_9Cl$ at 16 K. The emission of Sm^{2+} from sites II and IV is quenched at 80 and 220 K, respectively, and only emission from sites I and III can be observed at room temperature, in agreement with the two crystallographic sites available in the host lattice. With further increasing temperature, the intensity of the emission of Sm^{2+} in site I decreases sharply and is quenched at 450 K whereas site III still shows a strong emission. Due to thermal population, $4f^55d^1 \rightarrow 4f^6$ and $^5D_1 \rightarrow {}^7F_J$ transitions are observed at high temperature. The luminescence of Sm^{2+} is strongly temperature dependent in non-stochiometric hosts: At room temperature the emission spectra are composed of a broad band with a maximum at around 700 nm corresponding to the $4f^55d^1 \rightarrow 4f^6$ transition, while at 16 K, several groups of emission lines with a dominant line at 683.8 nm are observed. These emission lines are characteristic of the $^5D_0 \rightarrow {}^7F_J$ transitions of Sm^{2+}. Since the XRD patterns of both the stoichiometric and non-stoichiometric hosts are indistinguishable, it is still not clear which phases the Sm^{2+} ions occupy in the non-stoichiometric compounds.

Stoichiometric and non-stoichiometric compounds of Sm^{2+}-doped $Sr_2B_5O_9Cl$ and $Ca_2B_5O_9Cl$ were also prepared. The luminescence spectra of Sm^{2+} in stoichiometric $Sr_2B_5O_9Cl$ are composed of $4f^6 \rightarrow 4f^6$ emission lines. In contrast, in non-stoichiometric $Sr_2B_5O_9Cl$ the emission is characterized by $4f^55d^1 \rightarrow 4f^6$ broad band and $4f^6 \rightarrow 4f^6$ sharp line emission at room temperature and 16 K, respectively. The luminescence spectra of Sm^{2+} in $Ca_2B_5O_9Cl$ showed only broad band $4f^55d^1 \rightarrow 4f^6$ emission at all temperatures. The trend in the series $M_2B_5O_9Cl$ (M=Ba, Sr, Ca) is consistent with a decrease in the energy gap between the

$4f^5 5d^1$ and $^5D_0$ energy levels as the radii of the host metal ion decreases. This reflects an environment with an increasing ligand field, which increases the splitting of the 5d levels of the Sm^{2+} ions.

Acknowledgements

This work was supported by the Australian Research Council. We thank Dave Hunter for help with the DSC measurements.

References

1. Q. Zeng, N. Kilah, M.J. Riley, J. Lumin., in press.
P. Mikhail, J. Hulliger, M. Schnieper and H. Bill. *J. Mater. Chem.* **10** (2000), p. 987.
P. Mikhail, K. Ramseyer, G. Frei, F. Budde and J. Hulliger. *Opt. Commun.* **188** (2001), p. 111.
2. A. Meijerink and G. Blasse. *J. Phys. D: Appl. Phys.* **24** (1991), p. 626.
3. V. Dotsenko. *J. Mater. Chem.* **10** (2000), p. 561.
4. T.E. Peters and J. Baglio. *J. Inorg. Nucl. Chem.* **32** (1970), p. 1089.
5. M.D.J. Lloyd, A. Levasseur and C. Fouassier. *J. Solid State Chem.* **6** (1973), p. 179.
6. K. Machida, G. Adachi, N. Yasuoka, N. Kasai and J. Shiokawa. *Inorg. Chem.* **19** (1989), p. 3807.
7. V.P. Dotsenko, V.N. Radionoc and A.S. Voloshinovskii. *Mater. Chem. Phys.* **57** (1998), p. 134.
8. A. Meijerink and G. Blasse. *J. Lumin.* **43** (1989), p. 283.
9. R.D. Shannon. *Acta Cryst.* **A32** (1976), p. 751.
10. C. Wickleder. *J. Solid State Chem.* **162** (2001), p. 237.
C. Wickleder. *J. Lumin.* **94** (2001), p. 127.
11. Q. Zeng, Z. Pei, Q. Su and S. Lu. *Chem. Mater.* **11** (1999), p. 605.
12. H.V. Lauer, K.F. Fong, Jr. and J. Fong. *J. Chem. Phys.* **65** (1976), p. 3108.
13. Q. Zeng, Z. Pei, S. Wang, Q. Su and S. Lu. *J. Phys. Chem. Solids* **60** (1999), p. 515.
14. J.W.M. Verwey, G.J. Dirksen and G. Blasse. *J. Phys. Chem. Solids* **53** (1992), p. 367.
15. A. Lacam and C. Chateau. *J. Appl. Phys.* **66** (1989), p. 366.
16. J.D. Axe and P.P. Sorokin. *Phys. Rev.* **130** (1963), p. 945.
17. P. Dorenbos. *J. Lumin.* **91** (2000), p. 155.